RESEARCH ARTICLE

A Novel PCA-Based Slug Flow Characterization Using Acoustic Sensing

ABDULMAJID LAWAL[1,2], **NAVEED IQBAL**[1,2],
AZZEDINE ZERGUINE[1,2], (Senior Member, IEEE),
MOHAMED NABIL NOUI-MEHIDI[3], **MOHAMED LARBI ZEGHLACHE**[3],
AND ALI A. AL-SHAIKHI[1,2]

[1]Electrical Engineering Department, King Fahd University of Petroleum and Minerals (KFUPM), Dhahran 31261, Saudi Arabia
[2]Center for Communication Systems and Sensing, King Fahd University of Petroleum and Minerals (KFUPM), Dhahran 31261, Saudi Arabia
[3]EXPEC Advanced Research Center, Saudi Aramco, Dhahran 31311, Saudi Arabia

Corresponding author: Abdulmajid Lawal (abdulmajid.lawal@kfupm.edu.sa)

ABSTRACT In a modern industrial process, the accurate measurement of two-phase flow signals is of vital importance for various purposes including condition-based monitoring of pipelines, the avoidance of costly material and environmental damages, and danger to the operational personnel. In this work, a novel blind approach for denoising two-phase liquid and gas flow in a horizontal liquid-gas pipe is proposed. This approach employs the structured signal subspace (SSS) method on the multichannel signal acquired from the transducers connected to the wall of the pipe. The proposed approach utilizes only the output observations from the sensor, i.e, the recorded signal, and does not require any knowledge of the input signal or the channel. The multichannel signals recorded are first pre-processed using the principal component analysis (PCA) and then the blind SSS method is used to denoise the input signal before estimating it. The numerical results showed that the proposed algorithm outperforms the state-of-the-art algorithms (SOTA) which includes the eigen value decoposition (EGD)-based method and the independent component analysis (ICA)-based method, while the proposed PCA-SSS method achieved a performance of $-22.7dB$ in the presence of Gaussian noise, the EGD and ICA acheived $-16.39dB$ and $-18.09dB$, respectively, showing the superiority of the proposed method. Similar analysis were performed in the presence of a non-Gaussian noise and colored noise and the proposed algorithm also outperformed the other methods. Hence, the PCA-SSS method can be used for a better characterization of a slug flow regime by exploiting the Toeplitz structure embedded in the signal vector acquired from the array of sensors via the communication model for denoising the two-phase flow, and does not rely on the knowledge of the input signal vector.

INDEX TERMS Two-phase flow, structured signal subspace, principal component analysis, Toeplitz structure.

I. INTRODUCTION

The design of different industrial equipment and multi-phase-flow pipelines calls for a detailed analysis of a two-phase flow. A two-phase flow often occurs in different modern industrial processes such as crude oil production, nuclear reactor, and others. One of the most important regimes in a two-phase flow system is the slug flow regime, where pockets of liquid and gas form alternatively in the pipe-flow system.

The associate editor coordinating the review of this manuscript and approving it for publication was Vicente Alarcon-Aquino.

Acoustic passive sensing is one several flow monitoring methods used to analyze and characterize this type of flow regimes. In it, each time a pocket of gas or liquid passes through a particular section of the pipeline, a different sound or flow noise is generated which can be collected by a pipeline-mounted microphone and used for flow regime identification and accurate sound interpretation.

In recent times, many researchers have worked extensively on related aspects including flow phase distribution, flow regimes, void fraction. However, accurately measuring the two-phase flow rate still poses a great challenge to engineers

and remains a challenging problem. In the oil and gas industry, the multi- phase measurements and flow characterization is essential for production monitoring, production allocation, well testing, and reservoir management. The work of [1] gives a detailed review of into the significance of three-phase flow measurement, the primary approaches and technologies for metering such complex flows, and an insightful assessment of the current state of available solutions in this domain. The operators' understanding and use of the integration of Multi-phase Flow Meters (MFM) as a crucial measure for maximizing the potential of marginal fields is well explained in [2]. This prompted us to suggest here a new approach for the development of the next generation MFM capable of tackling yet-unsolved problems.

One main aspect of flow monitoring is determining the type of flow regime in the pipe, in difficult situations, such in oil and gas pipelines, where visual access is not possible. The type of flow regime can affect the operation and be harmful in cases of unwanted slug flow regimes. Slug flows have proved to be difficult to handle in multi-phase flow measurement, due to the intermittent nature of its flow condition where pockets of gas and liquid flow alternatively in a random way.

The literature is replete with a wide variety of techniques for slug flow measurement, including the electrical impedance technique [3], ultrasonic methods [4], radiation attenuation methods [5], and optical and video methods [6]. The work in [7] focuses on the hydrodynamic characteristics of slug flow in gas-liquid piping by using a capacitive probe for dynamic measurements in horizontal air-water slug flows, analyzing signals to characterize different flow regimes through Power Spectrum Density (PSD) and Probability Density Function (PDF) analysis.

Another promising technique for monitoring two-/multi-phase flow, widely used in industry, is the electrical resistance tomography (ERT). Dong et al. [8] combine the dual-plane ERT system with the cross-correlation method to measure a two-phase gas-liquid flow where the continuous phase is a conductive liquid. Hanus et al. [9] proposed the use of three main flow regimes, namely plug, bubble, and transitional plug-bubble, and employed the time- and frequency-domain signal features, to build an artificial neural network that recognizes a two-phase flow in a horizontal pipeline. Also, the principal component analysis (PCA) is used to reduce the number of features needed [10].

Though the literature shows that numerous researchers have worked on two-phase flow measurements using different techniques, the deleterious effect of the noise corrupting the sensors' flow measurements, on the accuracy of the two-phase flow rate measurement, did not receive adequate attention. As such, obtaining an accurate two-phase flow measurement remains a challenging task in the face of the corrupting noise emerging either from sensor measurements and/or from the noisy environment surrounding the flow system itself. Hence, given its importance in ensuring an accurate flow rate measurement, reducing the level of noise in the measurement via a pre-processing stage is a much-needed

task in a two-phase measurement. This is bound to greatly improve flow rate measurement accuracy and bring about other concomitant advantages.

This work proposes a new general framework for denoising multichannel two-phase liquid and gas acoustic signals collected from passive pipeline wall-mounted acoustic sensors. This requires neither prior knowledge of the input signal and the channel nor the noise level. Consequently, in our work, flow mass or rate is not measured, and only the noise collected from a slugging flow regime is identified to describe the frequency of the slugs and to filter any noise not related to the flow system. The proposed method first employs the PCA to denoise the multichannel signals and then uses the structured signal subspace (SSS) method to estimate the input signals from the sensors, as these are used for the estimation of the required flow characteristics based on the observed flow regime. Particular attention is given to the slug flow regime, in which pockets of gas and liquid flow alternatively. For the treatment of the acoustic signals measured, the prime motivation for using a blind approach here stems from the fact that, in this study, only the output signals from the sensors are assumed available, as is widely expected in practice where the user has no prior knowledge about either the signal input or the channel. Therefore, our adoption of the blind approach is very well justified as it accurately characterizes the slugging flow regime generated. To the best of our knowledge, this is the first time that this method is applied to a physical system as considered here. The aim is to develop a simple and cost-effective method to detect and qualify slug flow regimes in industrial flow lines.

The main contributions of this work comprise the following:

- Detailed study of the blind structured subspace (SSS) approach which (a) exploits the Toeplitz structure embedded in the signal vector acquired from the array of sensors via the communication model for denoising the two-phase flow, and (b) does not rely on prior knowledge of the input signal vector.
- Judicious exploitation of the advantages of the PCA technique to reduce the dimensionality of the received signal vector and the power of the blind SSS approach to build a workflow that effectively denoises the two-phase flow signal without any dependence whatsoever on the input knowledge.
- Development of an effective workflow to analyze both the synthetic data set and the real data set.

The novelty of our proposed blind SSS approach stems from its first-ever application to a practical problem, and its effectiveness, in terms of noise impact mitigation, enhanced signal quality and overall accuracy, in the face of an incomplete information about the two-phase flow in real-world scenarios. Hopefully, this will usher in a new research area in the field of measurement.

In this manuscript, the notations $()^H$, $()^T$, $()^*$, $()^{-1}$, $Tr()$ represent the conjugate transpose, the transpose, the conjugate, the inverse and the trace operations, respectively.

Bold lowercase alphabet $\boldsymbol{a}$ represents a vector, bold uppercase alphabet $\boldsymbol{A}$ represents a matrix, $\| \cdot \|^2$ and $\| \cdot \|_F^2$ represent the Euclidean and Frobenius norms, respectively, $\boldsymbol{I}_b$ represents an identity matrix of size $b \times b$ and $\boldsymbol{0}_{a,b}$ is an all-zero matrix of size $a \times b$. $a(i,j)$ and $Re()$ refer to the $(i,j)^{th}$ entry of matrix $\boldsymbol{A}$ and to the real part of a complex number, respectively.

The rest of the paper is organised as follows: Section II presents the system model, the principal component analysis, the structured signal subspace method, and the computational complexity. Section III explained the experimental setup used in this work. Section IV presents the results and their discussion. Finally, Section V concludes the paper.

II. THEORETICAL BASIS THE STRUCTURED SUBSPACE METHOD
A. SYSTEM MODEL
Consider a pipe in which multiple sensors are placed around a particular region in such a way that each sensor records the flowrate of the multiphase flow at a specific time interval. In this case, these multiple sensors concurrently record a multitude, or a vector, of signals at the same time instant through different channels. Thus, this signal acquisition system can be viewed as a single-input, multiple-output (SIMO) system with a single input signal passing through different channels, and resulting in multiple separate outputs that are recorded by different sensors.

Now, assume that each channel i in the SIMO measurement system, is linear with a discrete impulse response $h_i(k)$ and that each sensor measurement is corrupted by its associated noise $n_i(t)$. Then, at time t, the signal received by the ith sensor, as a result of the input signal $s(t)$ passing through its own i^{th} linear channel, with its discrete impulse response $h_i(k)$, will generate, through the channel's convolutive effect, the output $y_i(t)$ which can be modelled as follows:

$$y_i(t) = \sum_{k=0}^{L} h_i(k)s(t-k) + n_i(t), \quad t = 0, \ldots, N-1. \quad (1)$$

Here, N represents the data size and L represents the channel order. The channel-specific model in (1) can now be expanded to a system-wide model to cover the entire SIMO system, by rewriting (1) in a vector form so as to capture all of the available M sensor outputs into a single output vector $\boldsymbol{y}(t)$ modelled as follows:

$$\boldsymbol{y}(t) = \sum_{k=0}^{L} \boldsymbol{h}(k)s(t-k) + \boldsymbol{n}(t), \quad (2)$$

where

$$\boldsymbol{y}(t) = [y_1(t), y_2(t), \ldots, y_M(t)]^T, \quad (3)$$
$$\boldsymbol{h}(k) = [h_1(k), h_2(k), \ldots, h_M(k)]^T, \quad (4)$$

and

$$\boldsymbol{n}(t) = [n_1(t), n_2(t), \ldots, n_M(t)]^T. \quad (5)$$

Assuming that a window of W samples is taken by stacking the data into a vector/matrix representation, the model can now take its matrix form as follows:

$$\boldsymbol{y}_W(t) = \boldsymbol{H}_W \boldsymbol{s}_K + \boldsymbol{n}_W(t), \quad (6)$$

where $K = W + L$,

$$\boldsymbol{y}_W(t) = [\boldsymbol{y}^T(t), \ldots, \boldsymbol{y}^T(t-W+1)]^T, \quad (7)$$
$$\boldsymbol{s}_{W+L}(t) = [s(t), \ldots, s(t-K+1)]^T, \quad (8)$$

and $\boldsymbol{n}_W(t)$ is stacked in a similar fashion as $\boldsymbol{y}_W(t)$ and $\boldsymbol{H}_W$ is an $MW \times K$ block Toeplitz matrix defined as:

$$\boldsymbol{H}_W = \begin{bmatrix} \boldsymbol{h}(0) & \cdots & \boldsymbol{h}(L) & & \boldsymbol{0} \\ & \ddots & & \ddots & \\ \boldsymbol{0} & & \boldsymbol{h}(0) & \cdots & \boldsymbol{h}(L) \end{bmatrix}. \quad (9)$$

Now, consider N data samples, the following will hold:

$$\begin{aligned} \boldsymbol{Y} &= [\boldsymbol{y}_W(W-1) \; \boldsymbol{y}_W(W) \cdots \boldsymbol{y}_W(N-1)] \\ &= \boldsymbol{H}_W \boldsymbol{S}_K + \boldsymbol{N}_W, \end{aligned} \quad (10)$$

where

$$\boldsymbol{S}_K = \begin{bmatrix} s(W-1) & s(W) & \cdots & s(N-1) \\ s(W-2) & s(W-1) & \cdots & s(N-2) \\ \vdots & \vdots & & \vdots \\ s(W-K) & s(W-K+1) & \cdots & s(N-K) \end{bmatrix} \quad (11)$$

$\boldsymbol{S}_K$ is the signal's Hankel matrix of dimension $K \times (N-W+1)$.

B. PROPOSED PCA-SSS METHOD
The proposed principal component analysis PCA-based structured signal subspace (SSS) framework for denoising two-phase multichannel signals takes advantage of the PCA method's benefits for signal denoising while simultaneously leveraging the SSS method's capacity to blindly estimate the input signal without previous knowledge of the input signals. The fundamental reason for using the SSS technique is that in actuality, the user only has access to the noisy output signal from the sensors. Hence, the SSS can effectively deal with such situations by estimating the actual input in a blind context. It is worth mentioning that the SSS method has been applied to both linear [11] and nonlinear [12] systems. Therefore, the SSS is capable of handling nonlinear dynamics present in the two-phase multichannel signal. The denoising PCA-SSS framework block diagram is depicted in Fig. 1. In the first stage, PCA is applied to the multichannel signals collected from the sensors, significantly reducing the noise level in the signal. After that, the output of the PCA stage is sent to the SSS stage where the SSS is performed to extract the input signal and further reduce the noise level while retaining most of the features. Finally, the output of the SSS stage is made available at the output. Note also that to the best of our knowledge, this type of signal analysis has not been applied previously in similar studies.
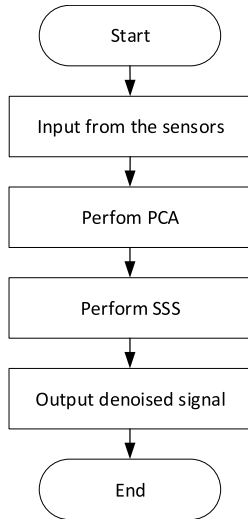
FIGURE 1. The flow chart of the proposed approach.

C. THE PRINCIPAL COMPONENT ANALYSIS

The overall procedure involves a hybrid method that employs the PCA and the blind SSS method to denoise the multichannel two-phase signal obtained by mounting several sensors on the pipe's surface. It is worthy of note that the PCA has been widely applied in different disciplines such as pattern recognition and signal processing [9], [13], [14], [15], [16], [17] to denoise signals. To achieve this aim, the signal is first transformed into the PCA domain so as to preserve the most vital principal components and eliminate the noisy ones. The literature has recently witnessed the emergence of several PCA-based approaches for denoising, especially in image processing. For example, the authors in [18] proposed an adaptive denoising approach that employs a PCA-transform-domain variation to preserve the local variation in the textures of the image. The authors in [19] proposed a denoising workflow that uses super-pixel grouping and PCA. The PCA transform is used to factorize similar patches and then estimate it through coefficient shrinkage in the PCA domain. To improve denoising performance and visualization details in image data, the authors in [20] used a cluster-wise progressive PCA thresholding that works based on Marchenko-Pastur (MP) law of random matrix theory [21].

To compute the PCA of a multichannel signal, several steps are involved. In the first step, the signal vector obtained from each of the $\bar{M}$ sensors is combined to form a matrix $\hat{Y}$ of $\bar{M} \times N$ and centralized by subtracting its mean ($\boldsymbol{\mu}$) as follows:

$$\bar{Y} = \hat{Y} - \boldsymbol{\mu}, \qquad (12)$$

where $\boldsymbol{\mu} = E[\hat{Y}]$. In the next stage, the covariance matrix of $\bar{Y}$ is estimated according to:

$$C_y = E[\bar{Y}\bar{Y}^T]. \qquad (13)$$

Next, the symmetric covariance matrix is decomposed using the following Eigendecomposition relation:

$$C_y = P \Sigma_p P^H, \qquad (14)$$

where $\boldsymbol{P} = [\boldsymbol{p}_1, \boldsymbol{p}_2, \ldots, \boldsymbol{p}_{\bar{M}}]$ is an $\bar{M} \times \bar{M}$ matrix that consists of orthonormal Eigenvectors and $\boldsymbol{\Sigma}_p = \text{diag}[\sigma_1, \sigma_2, \ldots, \sigma_{\bar{M}}]$ represents a diagonal matrix that consists of all the eigenvalues in decreasing order, i.e., $\sigma_1 \geq \sigma_2 \geq \ldots \geq \sigma_{\bar{M}}$. The aim of the PCA is to obtain an orthonormal transformation matrix $\boldsymbol{\Phi} = \boldsymbol{P}^H$ that decorrelates the matrix $\bar{Y}$ into the new matrix of $Y = \boldsymbol{\Phi}\bar{Y}$. To denoise the signal, the first vital M Eigenvectors are used to form a transformation matrix, such that $\tilde{\boldsymbol{\Phi}} = [\boldsymbol{p}_1, \boldsymbol{p}_2, \ldots, \boldsymbol{p}_M]$ with $M < \bar{M}$. The transformed matrix is then applied to the $\bar{Y}$ matrix such that

$$Y = \tilde{\boldsymbol{\Phi}}\bar{Y} \qquad (15)$$

will be of the lower dimension $M \times N$. This transform is also called the optimal dimensionality reduction and is useful for dimension reduction as well as for noise removal. This is due to the fact that the signal energy is concentrated in a small subset of the PCA-transformed data, while the noise energy is spread out evenly over the whole dataset.

D. STRUCTURED SIGNAL SUBSPACE (SSS) METHOD

In this section, based on the recently developed algorithms [11], [22], [23], the step-by-step method involved in performing the structured subspace method is presented here again. Also, the procedure of applying it in this context is explained. Basically, the SSS method directly estimates the transmitted signal from a convolutive mixture in the presence of noise. The method does not require prior knowledge of either the channel's impulse response or the transmitted signal as it operates in a blind manner. The advantages of using the SSS method include avoiding delay ambiguities and channel inversion which could propagate errors.

The SSS also has an implementational simplicity which is one of the features that makes it very attractive to use. The first implementation step involves obtaining the SVD of the matrix Y as shown:

$$Y = U\Sigma_u V^H, \qquad (16)$$

where U is a matrix made of the left singular vector of dimension $MW \times MW$, Σ_u is a diagonal matrix whose diagonal elements are the decreasing singular values of dimension $MW \times (N - W + 1)$, and V represents a matrix that contains the right singular vectors of dimension $(N - W + 1) \times (N - W + 1)$. The second step involves forming a new $(W + L) \times (N - W + 1)$ matrix V_s that spans the rows subspace of the signal matrix in the noiseless case by taking the Hermitian transpose of the first $(W + L)$ columns of the matrix V.

Finally, the denoised signal is estimated as $\hat{S} = QV_s$. Here, the Q matrix of $(W + L) \times (W + L)$ is chosen such that the structure of the signal matrix is preserved. To achieve this,

the following cost function is devised: ($T = N - W + 1$, $P = MW$, and $K = W + L$):

$$J = \sum_{j=1}^{K-1} \sum_{i=1}^{T-1} \left| \hat{s}(i,j) - \hat{s}(i+1, j+1) \right|^2, \qquad (17)$$

where $\hat{s}(i,j)$, is the $(i,j)^{th}$ entry of the estimated signal matrix $\hat{S}$. This cost function is built based on the Hankel structure of the signal matrix given in (11) and can be expressed as:

$$J = \| J_K \hat{S}_K J_T - \tilde{J}_K \hat{S}_K \tilde{J}_T \|_F^2, \qquad (18)$$

where $J_K \hat{S}_K J_T$ and $\tilde{J}_K \hat{S}_K \tilde{J}_T$ are the top-left and right-bottom submatrices of $\hat{S}_K$, respectively. The first pair of selection matrices J_K and J_T are defined as: $J_K = \begin{bmatrix} I_{K-1} & 0_{(K-1),1} \end{bmatrix}$, where $0_{(K-1),1}$ is an all-zero column vector that contains zeros of dimension $(K-1) \times 1$, and I_{K-1} is a square identity matrix of size $(K-1)$, and $J_T = \begin{bmatrix} I_{T-1} & 0_{1,(T-1)} \end{bmatrix}^T$. As to the second pair of selection matrices $\tilde{J}_K$ and $\tilde{J}_T$, they are similarly defined as: $\tilde{J}_K = \begin{bmatrix} 0_{(K-1),1} & I_{K-1} \end{bmatrix}$ and $\tilde{J}_T = \begin{bmatrix} 0_{(T-1),1} & I_{T-1} \end{bmatrix}^T$.

Next, the Kronecker product property of $\text{vec}(ABC) = ((C^T \otimes A)\text{vec}(B)) = ((C^T \otimes A)b)$ is applied here to vectorize the cost function presented in (18), where $b = \text{vec}(B)$ and this leads to

$$J = \| \left((V_s J_T)^T \otimes J_K - (V_s \tilde{J}_T)^T \otimes \tilde{J}_K \right) \text{vec}(Q) \|^2$$
$$= \| Zq \|^2, \qquad (19)$$

where $Z = \left((V_s^H J_T)^T \otimes J_K - (V_s^H \tilde{J}_T)^T \otimes \tilde{J}_K \right)$ and $q = \text{vec}(Q)$.

The above optimization problem can be reformulated as follows:

$$J = \min_q \ q^H Z^H Z q. \qquad (20)$$

In this case, the smallest Eigenvalue of the matrix $Z^H Z$ corresponds to the Eigenvector which is the optimal solution q under the unit-norm constraint. The matrix Q is obtained by reshaping q into a $K \times K$ matrix. Hence, the estimated signal is given by $\hat{S}_K = QV_s$.

Finally, The step-by-step procedure involved in the proposed PCA-SSS method is described in Algorithm 1.

E. COMPUTATIONAL COMPLEXITY

In this section, the computational complexity of the proposed PCA-SSS method is presented. The sequence of steps involved in the processing of the proposed PCA-SSS method is detailed. The first stage of the proposed method involves performing the PCA operation: here the covariance matrix of $\bar{M} \times N$ dimension input data is calculated with a cost of $O(\bar{M}^2 N)$. Next, the eigen decomposition is calculated with a cost of $O(\bar{M}^3)$ followed by the M-dimensional principal component used to recover the data with a cost of $M\bar{M}N$.

In the second stage, the SSS is performed on the data: the first step of the SSS involves the SVD of the data matrix which is computed with a cost of $O(MW(N - W + 1)^2)$. Next,

---

Algorithm 1 Summary of the Proposed PCA-SSS Method

Obtain the signal from sensors $\tilde{Y}$
Perform the PCA:
$\bar{Y} = \tilde{Y} - \mu$
$C_y = E[\bar{Y}\bar{Y}^T]$
$C_y = P\Sigma P^H$
$\Phi = [p_1, p_2, \ldots, p_M]$
$Y = \Phi\bar{Y}$
Perform the SSS:
$Y = U\Sigma V^H$
$J = \| J_K QV_s J_T - \tilde{J}_K QV_s \tilde{J}_T \|^2$
$Z = (V_s^H J_T)^T \otimes J_K - (V_s^H \tilde{J}_T)^T \otimes \tilde{J}_K$
$J = \min_q \ q^H Z^H Z q$
Reshape q into a $K \times K$ matrix Q
Output Denoised Signal:
$\hat{S}_K = QV_s$
End

---

the computation of the Eigen decomposition of the $Z^H Z$ is performed with a cost of $O(K^3)$.

Finally, the overall cost of computational of the proposed PCA-SSS method is $O(\bar{M}^2 N) + O(\bar{M}^3) + O(MW(N - W + 1)^2) + O(K^3) + M\bar{M}N$.

Table 1 details the computational complexity of all the steps involved in the computation of the proposed PCA-SSS algorithm.

TABLE 1. The computational complexity of all the steps involved in the computation of the proposed PCA-SSS algorithm.

Sequence of Steps	Computational Complexity
Covariance matrix	$O(\bar{M}^2 N)$
Eigen decomposition	$O(\bar{M}^3)$
Data recovery	$M\bar{M}N$
SVD	$O(MW(N-W+1)^2)$
Eigen decomposition	$O(K^3)$
Total cost	$O(\bar{M}^2 N) + O(K^3) + M\bar{M}N + O(\bar{M}^3) + O(MW(N-W+1)^2)$

III. EXPERIMENTAL SETUP

The experimental setup considered in this study consists of a mixture of gas and liquid in a closed flow-loop. The flow-loop consists of a feed tank which is connected directly to a pump that operates with a variable speed drive (VSD). The pump is connected to an electromagnetic flowmeter and has a maximum capacity of $100 \ l/min$. The pipe flow has a 3-inch diameter and consists of two long sections; a 3-meter vertical test section and a 2-meter horizontal test section. The system diagram is depicted in Fig.2.

The flow in the pipe is returned back to the feed tank. It is important to note that compressed air is used as gas in the experiments. The air is produced by a central compression feed to the building with a delivery pressure of 10 bars and is injected just downstream to the flow meter at the inlet of the test section, with a check valve that prevents reversal

flow at the junction point. The flow is designed such that it allows for the analysis of rapidly-generated slugs during the experiment. The environmental temperature is highly controlled and held constant throughout the experiment. To ensure good coupling between the acoustic sensors and the pipe materials, an adhesive is used to securely position the acoustic sensor on the wall of the pipe. The acoustic sensor is a microphone (Knowles Mic Cond Analog) that can record in a frequency range of 280-5000 Hz. A National instrument multi-channel acquisition system that runs with LabView, is used to acquire the signal from the acoustic sensors at different acquisition rates. The signal is recorded under different flow regimes and at different superficial liquid and gas velocities controlled using a variable speed drive (VSD).

The flow measurements were performed for different flow conditions, the liquid rate measured with the flowmeter were ramped up from 10 l/min to 50 l/min, and for each liquid flow rate, the gas (compressed air) flow rates measured by a gas meter were ramped up from 10 l/min to 100 l/min. For each combination of liquid rate and gas rate, where a slugging flow is observed, the flow noise measurements are captured and treated.
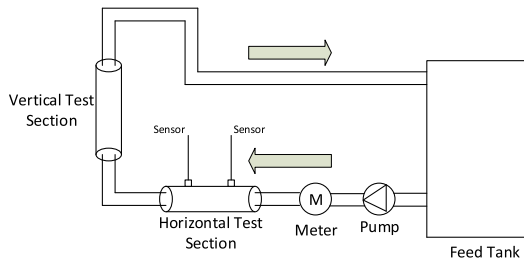

FIGURE 2. The block diagram of the experimental setup.

Figure 3 shows how a single microphone sensor is installed on the pipe-flow wall. For acoustic coupling purposes, a thin layer of silicon oil is applied to the microphone surface before attaching it to the pipe wall. Note that all experiments were conducted in a laboratory setup. There is no difference expected in the field since the observations are about changes in the noise collected from a flow in a pipeline. Although, the process noise might be present, in most cases the sensor reference floor will have the same components as the signals collected during the slugging phenomenon. Therefore, the changes are not significant between a controlled experimental system and a real pipeline flow system. Also, it is worth mentioning that here we are not following the mass flow change, since it cannot be measured with passive acoustic signals; we are following the slugs that are formed in the slug flow regime, i.e., the pockets of gas and liquids that alternately flow in the pipe. In addition, we are only tracing noise level change in the system, without analyzing the content.

IV. RESULTS AND DISCUSSIONS
In this section, the performance of the proposed algorithm based on the general procedure, discussed here, for denoising
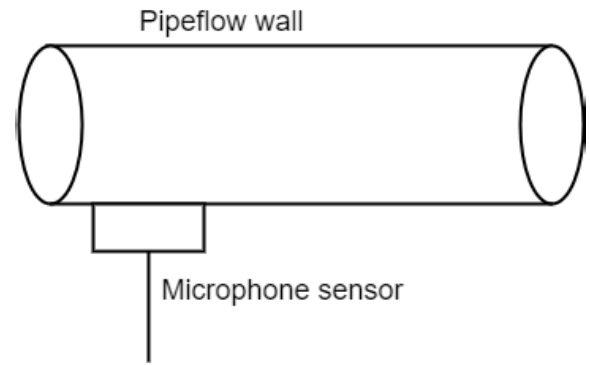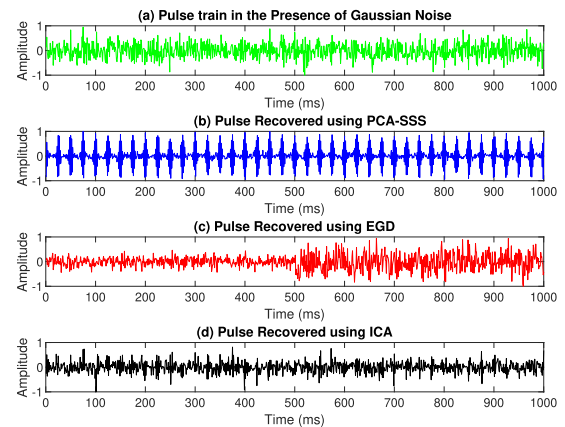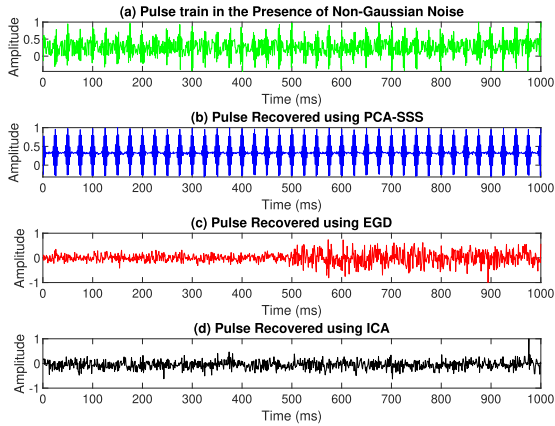

FIGURE 3. Sensors installation.

FIGURE 4. (a) The Gaussian pulse train in the presence of Gaussian noise, (b) the recovered Gaussian pulse train using PCA-SSS, (c) the recovered Gaussian pulse train using EGD, (d) the recovered Gaussian pulse train using ICA.

multichannel signals received from different sensors, is investigated. Specifically, this general procedure consists of the proposed hybrid method that employs the PCA and the blind SSS method for denoising multichannel two-phase signals obtained by placing multiple sensors on the surface of a pipe. In order to verify the effectiveness of the proposed technique, a simulated data set that represents the two-phase flow is generated. The generated data is a $0.5KHz$ Gaussian pulse [24] train of 30 percent bandwidth with a repetition frequency of $40Hz$, a sampling frequency of $1KHz$, and a pulse length of 14 seconds. Here, we assumed that $\bar{M} = 10$ sensors are available and each sensor receives $N = 14000$ samples. Hence, the input to the PCA is a 14000×10 dimensional data, the first $M = 2$ principal component are used for data recovery. As for the SSS method, the output of the PCA which has now a dimension of 14000×2 is passed to the SSS method which uses $W = 5, N = 14000$, and $M = 2$.

Figure 4 depicts a comparison of pulse recovery performance between the PCA-SSS method and several state-of-the-art (SOTA) techniques, such as the generalized eigenvalue decomposition (EGD) [25] and the independent component analysis (ICA) [26], under the influence of Gaussian noise. it is crucial to emphasize that the Joint Approximation Diagonalization of Eigenmatrices (JADE)

ICA method is used in this case. Notably, the PCA-SSS method demonstrates superior signal recovery capabilities when compared with these SOTA approaches.

In the subsequent analysis, we evaluate the performance of PCA-SSS in comparison to EGD and ICA under the influence of non-Gaussian noise, specifically, a uniformly distributed noise in the range [0, 1], as illustrated in Fig. 5. Remarkably, in this particular setting, the PCA-SSS demonstrates its superiority by achieving better signal recovery results when compared to these SOTA algorithms.

FIGURE 5. (a) The Gaussian pulse train in the presence of Non-Gaussian (Uniform) noise, (b) the recovered Gaussian pulse train using PCA-SSS, (c) the recovered Gaussian pulse train using EGD, (d) the recovered Gaussian pulse train using ICA.

In the context of colored noise, the performance of the PCA-SSS method surpasses both EGD and ICA, showing its effectiveness in denoising signals within this specific scenario as depicted in Fig. 6.
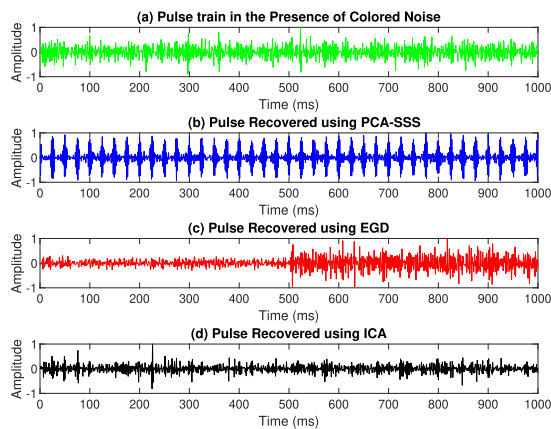
FIGURE 6. (a) The Gaussian pulse train in the presence of colored noise, (b) the recovered Gaussian pulse train using PCA-SSS, (c) the recovered Gaussian pulse train using EGD, (d) the recovered Gaussian pulse train using ICA.

To quantitatively compare the PCA-SSS method to the other SOTA approaches, the mean squared error metric is employed which is given in dB as:

$$\text{MSE}(dB) = 10 \log_{10} \left(\frac{1}{N_L} \sum_{i=1}^{N_L} \| \hat{s}_i - s \|_2^2 \right). \quad (21)$$

Table 2 provides a summary of the quantitative outcomes derived from the examination of the PCA-SSS method, the EGD-based method, and the ICA-based method when subjected to Gaussian, non-Gaussian, and colored noise for a signal-to-noise ratio of 0dB. The results reveal that, regardless of the noise type, the PCA-SSS method outperforms the rest of the methods. To further support this assessment, Fig. 7 illustrates a comparative analysis of the proposed PCA-SSS, EGD, and ICA methods interms of MSE versus SNR. This addresses the effectiveness of the proposed PCA-SSS method for a wide range of SNR variations.

**TABLE 2.** The MSE for different algorithms in the presence of different types of noise.

Noise	PCA-SSS	EGD	ICA
Gaussian	-22.76dB	-16.39dB	-18.09dB
Non-Gaussian	-3.15dB	-1.53dB	-1.04dB
Colored	-38.54dB	-27.10dB	-32.48dB
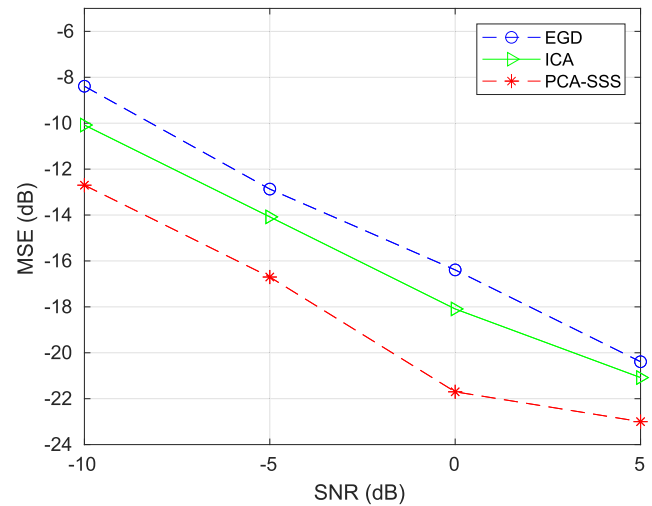
FIGURE 7. The MSE versus SNR.

While Fig. 8 (a) depicts the first 300 samples of the complete data set of the 14,000 samples and of $W = 5$, Fig. 8 (b) shows its noisy Gaussain version. We observe that the simulated noisy signal is not visually recognizable after it has been completely mixed with noise, thus reflecting a real-life noise-corrupted signal.

To recover the original input signal, the proposed algorithm is applied to the noisy multichannel output. First, the PCA is applied and the recovered Gaussian pulse train using PCA is shown in Fig. 8 (c). It can be observed from this figure, that the PCA could not completely recover the signal efficiently. This is expected as the PCA removes only the noise affecting the features that were cut out but preserve the noise in the features that have been retained. As such, the recovered signal remains noisy and has artifacts caused by the PCA's truncation effect in the feature domain. Hence, the PCA alone cannot effectively denoise the received signal. Next, the proposed PCA-SSS method is applied to the noisy signal. As illustrated in Fig. 8 (d), the proposed algorithm effectively
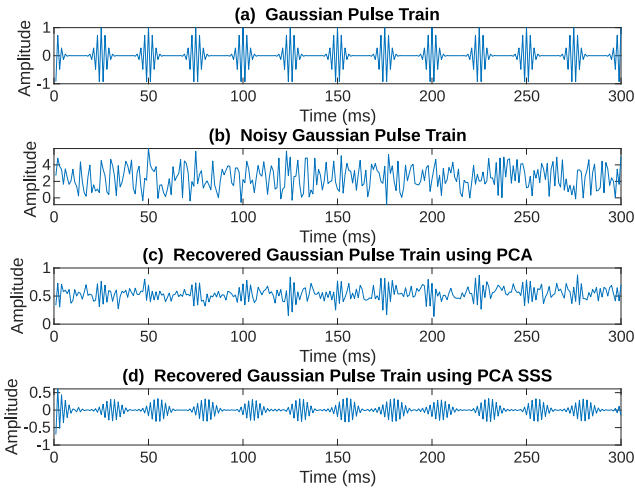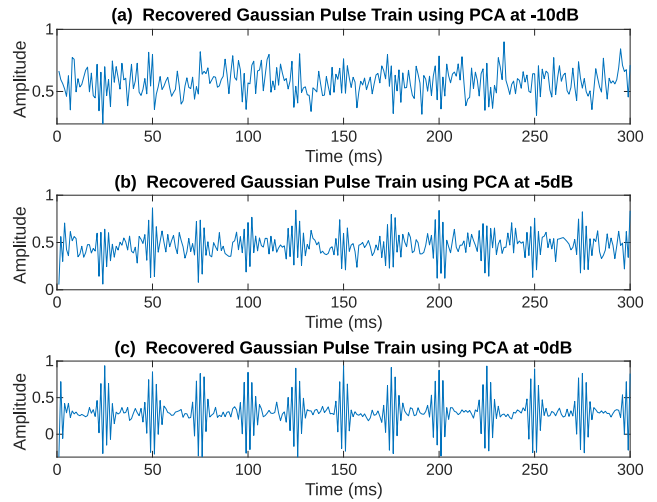
FIGURE 8. (a) The noiseless Gaussian pulse train, (b) the noisy Gaussian pulse train, (c) the recovered Gaussian pulse train using PCA, (d) the recovered Gaussian pulse train using PCA-SSS method.

FIGURE 9. The recovered Gaussian pulse train using PCA at different SNRs.

denoised the signal and recovered the original noiseless signal. This clearly proves that the proposed algorithm is robust and capable of effectively and efficiently denoising the received noisy signal. The amplitude disparity between the recovered Gaussian pulse train using the proposed PCA-SSS method and the original Gaussian pulse train signal in terms of amplitude is due to the scalar ambiguity inherent in the blind processing technique as well as the filtering effect. It is worth noting that all blind processing techniques have scalar ambiguity.

To quantify the level of noise and understand the extent to which the algorithm can perform well, the PCA is employed to recover the original pulse train at different SNR levels of $-10dB$, $-5dB$ and $0dB$ as shown in Fig. 9. Obviously, at $-10dB$, the PCA could not recover any meaningful information from the noisy pulse train signal since, at this very low SNR, the pulse train is severely corrupted by the added noise. Also, at the low SNR of $-5dB$, the PCA managed to recover a noisy version of the original signal that bears a reasonable resemblance to it, but still contains a significant amount of noise. Finally, at $0dB$, the PCA recovered the signal containing a high degree of information from the original pulse train. At this stage, it is worth recalling that the PCA has been designed to reduce noise but not eliminate it altogether. Hence, as expected, we can notice here that the performance of the PCA improves as the SNR increases.

In Fig. 10, a similar analysis is performed using the proposed PCA-SSS method so as to demonstrate the efficacy of the SSS in removing the noise leftover from the PCA, even in very noisy environments characterized by very low SNRs. It can be noted from Fig. 10 (a) that, in the very low SNR case of $-10dB$, the Proposed PCA-SSS method has managed to noticeably outperform the PCA only scheme in that, the envelope of the recovered signal bears a close resemblance to that of the original pulse train, except for some amount of noise-induced amplitude scaling and a slightly

higher amplitude of the peak of the initial pulse due probably to some noise-induced transient behavior of the proposed technique.

A similar remarkable improvement brought about by the PCA-SSS method at both $-5dB$ and $0dB$ is also depicted in Fig. 10 (b) and (c), respectively, thus leading to the conclusion that the proposed combined PCA-SSS method has undeniably outperformed the conventional PCA method in denoising multichannel signals even in very low SNRs environments.
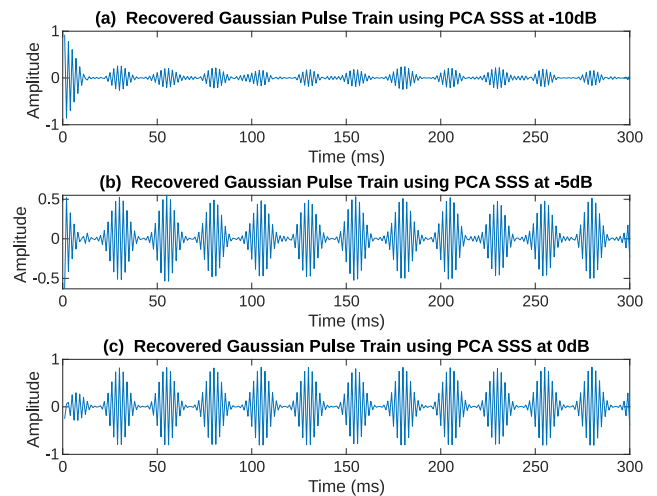

FIGURE 10. The recovered Gaussian pulse train using the PCA-SSS method for different SNRs.

In the next stage, we investigate the frequency content of the generated original pulse train in the noiseless case, the noisy signal, and the recovered signal using the proposed PCA-SSS method. Figure 11 illustrates the repetition frequency (slug flow frequency) of the generated noiseless synthetic data, its noisy version, and that of the recovered signal. The frequency range of the recovered signal corresponds to that of the original signal, the amplitude of the recovered signal differs somewhat from that of the recovered

signal and this may be due to the scalar ambiguity inherent in the SSS blind algorithms.
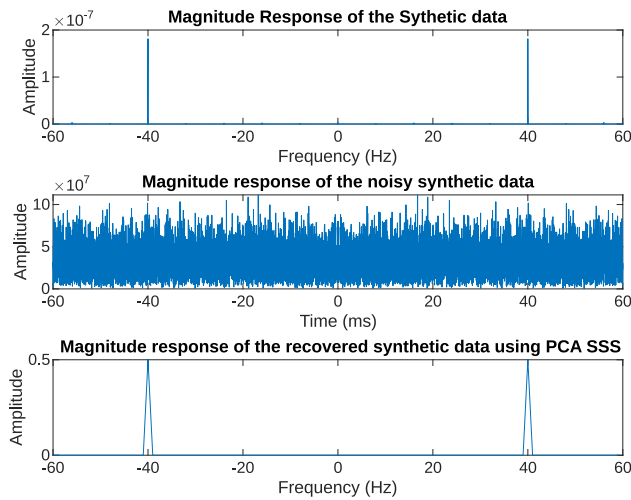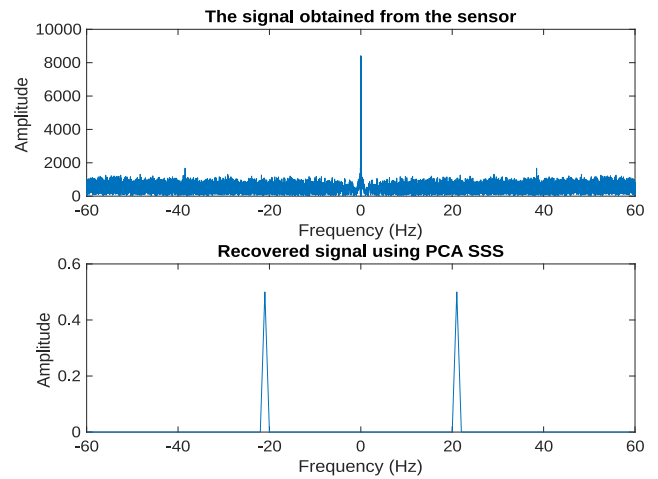

FIGURE 11. The frequency response of the noiseless synthetic data, noisy synthetic data, and recovered synthetic data using PCA-SSS method.
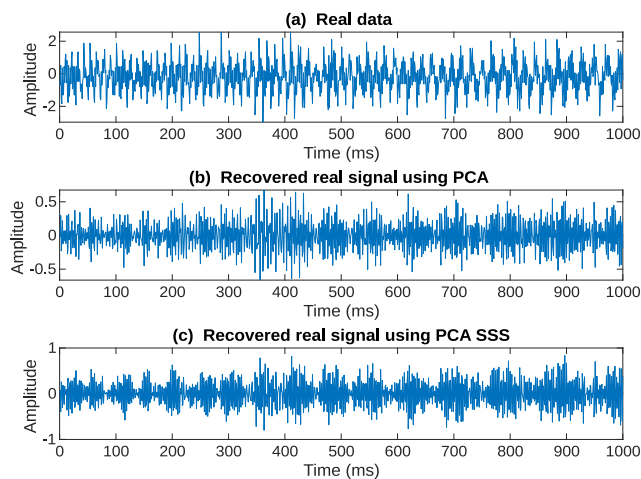
FIGURE 12. (a) The real noisy signal recorded from the sensors, (b) the recovered signal using PCA, and (c) the recovered signal using PCA-SSS method.

Next, after validating the proposed PCA-SSS method with the generated synthetic data, the method is applied to a real data scenario obtained from the M different sensors placed on the wall of the pipe. The signals are recorded simultaneously from the sensors while the two-phase liquid flows along the pipe. The received signal is a multichannel signal with each sensor receiving its signal from its own separate channel. While Fig. 12 (a) depicts the original noisy signal, Fig. 12 (b) shows the results of applying only the PCA to the real multichannel signal. We observe that the PCA-recovered signal is quite noisy, random like, and does not reveal any specific trend. Ultimately, in Fig. 12 (c), the denoised signal using the developed PCA-SSS method is illustrated. Thus, comparing the outputs of the PCA-only, with that of the proposed PCA-SSS method, clearly shows that the latter method is highly effective and superior to the former one in

FIGURE 13. The frequency response of the real noisy signal recorded from the sensors, and that of the recovered signal using PCA-SSS method.

denoising the signal. Note also that this superiority has also been shown earlier at very low SNRs.

Finally, the frequency content of the real noisy signal and its recovered version using the proposed PCA-SSS method is depicted in Fig. 13. The slug flow frequency, which is of interest to us, is seen in the magnitude spectrum of the recovered signal using the PCA-SSS method.

V. CONCLUSION

A novel approach for denoising the sensors' output signals in a multichannel two-phase liquid and gas has been proposed and developed in this paper. The proposed approach offers a new solution to the two-phase liquid/gas flow problem which is of paramount importance in several industrial applications as clearly explained in the Introduction Section. Such signals are invariably plagued with unavoidable noise signals, particularly in industrial settings. Moreover, the channel input and impulse response are rarely known or may require extra techniques for their separate estimation. This therefore calls for the use of efficient estimation techniques that avoid these two problems. Our approach, as shown in this work, was designed to plug these two gaps in the current literature by tackling these two unavoidable difficulties and offering an efficient solution to the multi-channel two-phase flow problem.

Our approach exploits the intrinsic powers of the PCA and the SSS methods and combines them into a single new PCA-SSS method to first denoise the signal received from multiple sensors attached to the wall of the pipeline carrying a two-phase liquid-gas fluid. As such, it uses the PCA as a pre-processing stage to reduce the noise level, before feeding the resulting "cleaned" signal to the SSS stage to remove the remaining amount of noise and efficiently denoise the received signal so as to recover the original one. Our method showed that the powerful SSS technique, whilst doing away with the knowledge of either the input signal or the channel's impulse response, and hence operating in a completely blind manner, derives its signal denoising power from exploiting the Toeplitz structure present in the signal matrix.

The effectiveness, robustness, and power of the proposed method were proven through its successful application to a synthetic signal and then to a real one to emphasize its practical application in real-world applications. It was clearly demonstrated that the proposed combined PCA-SSS method significantly outperforms the conventional PCA-only method, in denoising a noisy multi-channel signal from a two-phase flow, and can even exhibit a reasonable performance even in very-low-SNR environments, where the PCA-only method remains totally powerless and hopelessly ineffective. This satisfactory noise-related performance in very-low SNR scenarios further illustrates the applicability of our proposed multi-channel two-phase method to real-world applications. The results obtained under various SNR levels and for both synthetic and real signals corroborate very well the theoretical underpinnings of the proposed method and thus give ample encouragement for embedding this new technique in modern flowmeters to greatly enhance their flow rate estimation accuracy. Moreover, the present work will offer a simple and easily implemented method, and tool to better detect slugging flows when they occur in a non-transparent pipe flow such as in real industrial systems. Another added advantage of the proposed method is its use, in real-world applications, as a low-cost detection method that can guide and help the operator take decisions to better manage the event of unwanted slug flow regimes, thus improving the overall efficiency and performance of the system and reducing its energy consumption and running cost.

Additionally, in practical real-world applications where ground truth is unavailable, we firmly believe that use of the blind approach, as demonstrated in this work, is the "go-to" approach as it assumes, at its core, either the total lack, or at best very little, of the ground truth, specifically the information of the quality of the inputs impinging on the process and the noise corrupting them and whether these are either of the colored Gaussian or non-Gaussian types.

As such, the blind approach adopted in our study makes its performance hardly sensitive to the quality of the input data and, instead, draws all of its needed data from the received outputs thanks to its use of the blind SSS technique. It is important to note here that the experimental data used in this paper emanate from an operational scenario that is commonly found in real-world applications. As such, the results obtained for this practical operational scenario provide a reliable prediction of the expected performance of our proposed method.

Finally, all of the above-mentioned attractive practical features of our proposed method amply demonstrate its practical applications to real-world multi-channel two-phase problems.

ACKNOWLEDGMENT

REFERENCES

[1] R. Thorn, G. A. Johansen, and E. A. Hammer, "Recent developments in three-phase flow measurement," *Meas. Sci. Technol.*, vol. 8, no. 7, pp. 691–701, Jul. 1997.

[2] G. Falcone, G. F. Hewitt, C. Alimonti, and B. Harrison, "Multiphase flow metering: Current trends and future developments," in *Proc. SPE Annu. Tech. Conf. Exhib.*, Sep. 2001, p. 71474.

[3] M. Fossa, G. Guglielmini, and A. Marchitto, "Intermittent flow parameters from void fraction analysis," *Flow Meas. Instrum.*, vol. 14, nos. 4–5, pp. 161–168, Aug. 2003.

[4] H. Murakawa, H. Kikura, and M. Aritomi, "Application of ultrasonic multi-wave method for two-phase bubbly and slug flows," *Flow Meas. Instrum.*, vol. 19, nos. 3–4, pp. 205–213, Jun. 2008.

[5] M. J. S. King, C. P. Hale, C. J. Lawrence, and G. F. Hewitt, "Characteristics of flowrate transients in slug flow," *Int. J. Multiphase Flow*, vol. 24, no. 5, pp. 825–854, Aug. 1998.

[6] R. van Hout, D. Barnea, and L. Shemer, "Translational velocities of elongated bubbles in continuous slug flow," *Int. J. Multiphase Flow*, vol. 28, no. 8, pp. 1333–1350, Aug. 2002.

[7] E. dos Reis and L. Goldstein, "Characterization of slug flows in horizontal piping by signal analysis from a capacitive probe," *Flow Meas. Instrum.*, vol. 21, no. 3, pp. 347–355, Sep. 2010.

[8] F. Dong, Y. Xu, L. Hua, and H. Wang, "Two methods for measurement of gas-liquid flows in vertical upward pipe using dual-plane ERT system," *IEEE Trans. Instrum. Meas.*, vol. 55, no. 5, pp. 1576–1586, Oct. 2006.

[9] R. Hanus, M. Zych, L. Petryka, D. Świsulski, and A. Strzępowicz, "Application of ANN and PCA to two-phase flow evaluation using radioisotopes," in *Proc. EPJ Web Conf.*, vol. 143, 2017, p. 02033.

[10] Y. Ju, Z. Cui, and Q. Xiao, "Fault diagnosis of power plant condenser with the optimized deep forest algorithm," *IEEE Access*, vol. 10, pp. 75986–75997, 2022.

[11] A. Lawal, Q. Mayyala, K. Abed-Meraim, N. Iqbal, and A. Zerguine, "Blind signal estimation using structured subspace technique," *IEEE Trans. Circuits Syst. II, Exp. Briefs*, vol. 68, no. 8, pp. 3007–3011, Aug. 2021.

[12] A. Lawal, K. Abed-Meraim, A. Zerguine, Q. Mayyala, and A. Muqaibel, "Semi-blind structured subspace method for signal estimation in non-linear convoluted mixture," *Signal Process.*, vol. 210, Sep. 2023, Art. no. 109084.

[13] M.-J. Wu, Y.-L. Gao, J.-X. Liu, C.-H. Zheng, and J. Wang, "Integrative hypergraph regularization principal component analysis for sample clustering and co-expression genes network analysis on multi-omics data," *IEEE J. Biomed. Health Informat.*, vol. 24, no. 6, pp. 1823–1834, Jun. 2020.

[14] H. Roopa and T. Asha, "A linear model based on principal component analysis for disease prediction," *IEEE Access*, vol. 7, pp. 105314–105318, 2019.

[15] Z. Kai, L. Daojing, C. Anjing, H. Dong, T. He, Y. Haifeng, D. Jianbo, L. Lei, Z. Yu, and Z. Running, "Sparse flight spotlight mode 3-D imaging of spaceborne SAR based on sparse spectrum and principal component analysis," *J. Syst. Eng. Electron.*, vol. 32, no. 5, pp. 1143–1151, Oct. 2021.

[16] Q. Guo, T. Pan, S. Chen, X. Zou, and D. Y. Huang, "A novel edge effect detection method for real-time cellular analyzer using functional principal component analysis," *IEEE/ACM Trans. Comput. Biol. Bioinf.*, vol. 17, no. 5, pp. 1563–1572, Sep. 2020.

[17] Y. Hu, J.-X. Liu, Y.-L. Gao, and J. Shang, "DSTPCA: Double-sparse constrained tensor principal component analysis method for feature selection," *IEEE/ACM Trans. Comput. Biol. Bioinf.*, vol. 18, no. 4, pp. 1481–1491, Jul. 2021.

[18] W. Zhao, Q. Liu, Y. Lv, and B. Qin, "Texture variation adaptive image denoising with nonlocal PCA," *IEEE Trans. Image Process.*, vol. 28, no. 11, pp. 5537–5551, Nov. 2019.

[19] S. R. S. P. Malladi, S. Ram, and J. J. Rodríguez, "Image denoising using superpixel-based PCA," *IEEE Trans. Multimedia*, vol. 23, pp. 2297–2309, 2021.

[20] W. Zhao, Y. Lv, Q. Liu, and B. Qin, "Detail-preserving image denoising via adaptive clustering and progressive PCA thresholding," *IEEE Access*, vol. 6, pp. 6303–6315, 2018.

[21] J. Veraart, E. Fieremans, and D. S. Novikov, "Diffusion MRI noise mapping using random matrix theory," *Magn. Reson. Med.*, vol. 76, no. 5, pp. 1582–1593, Nov. 2016.

[22] Q. Mayyala, K. Abed-Meraim, and A. Zerguine, "Structure-based subspace method for multichannel blind system identification," *IEEE Signal Process. Lett.*, vol. 24, no. 8, pp. 1183–1187, Aug. 2017.

[23] A. Lawal, Q. Mayyala, K. Abed-Meraim, N. Iqbal, and A. Zerguine, "Toeplitz structured subspace for multi-channel blind identification methods," *Signal Process.*, vol. 188, Nov. 2021, Art. no. 108152.

[24] C. Bauer, R. Freeman, T. Frenkiel, J. Keeler, and A. Shaka, "Gaussian pulses," *J. Magn. Reson.*, vol. 58, no. 3, pp. 442–457, 1969.

[25] L. Zhou and C. Li, "Outsourcing eigen-decomposition and singular value decomposition of large matrix to a public cloud," *IEEE Access*, vol. 4, pp. 869–879, 2016.

[26] G. Sahonero-Alvarez and H. Calderon, "A comparison of SOBI, FastICA, JADE and infomax algorithms," in *Proc. 8th Int. Multi-Conf. Complex., Inform. Cybern.*, Mar. 2017, pp. 17–22.

ABDULMAJID LAWAL received the B.Eng. degree in electrical engineering from Bayero University, Kano, in 2012, and the master's and Ph.D. degrees in electrical engineering from the King Fahd University of Petroleum and Minerals (KFUPM), Saudi Arabia, in 2016 and 2021, respectively. He is currently a Postdoctoral Fellow Student with the Center for Communication Systems and Sensing, KFUPM. He focuses on issues with blind source separation, blind system/channel identification, sparse signal representations, and artificial intelligence. His research interests include statistical signal processing, modeling, estimation, and the classification of signals.

NAVEED IQBAL received the B.S. and M.S. degrees in electrical engineering from the University of Engineering and Technology Peshawar, Peshawar, Pakistan, and the Ph.D. degree from the King Fahd University of Petroleum and Minerals (KFUPM), Saudi Arabia. He is currently a Research Associate Professor with KFUPM. His research interests include adaptive algorithms, compressive sensing, heuristic algorithms, and seismic signal processing, machine learning, and data acquisition networks. He has more than 30 publications in international journals/conferences and nine patents in the aforementioned areas.

AZZEDINE ZERGUINE (Senior Member, IEEE) received the B.Sc. degree in electrical engineering from Case Western Reserve University, Cleveland, OH, USA, in 1981, the M.Sc. degree in electrical engineering from the King Fahd University of Petroleum and Minerals (KFUPM), Dhahran, Saudi Arabia, in 1990, and the Ph.D. degree in electrical engineering from Loughborough University, Loughborough, U.K., in 1996. He is currently a Professor with the Department of Electrical Engineering, KFUPM, working in the areas of signal processing and communications. His current research interests include signal processing for communications, adaptive filtering, neural networks, the applications of artificial intelligence, blind source separation, and blind equalization. He was a recipient of the three Best Teaching Awards at KFUPM, in 2000, 2005, and 2011, and the Best Research Award at KFUPM, in 2017. He is also serving as an Associate Editor for the *Signal Processing* journal and the *EURASIP Journal on Advances in Signal Processing*.

MOHAMED NABIL NOUI-MEHIDI received the Ph.D. degree in energy systems from Kobe University, Japan, in 2002. He spent ten years teaching in academia before working for the Commonwealth Scientific and Industrial Research Organization (CSIRO) in Australia. He has been with Saudi Aramco Oil Company, since 2008. His main research interests include industrial fluid dynamics, oil and gas production, fluid sensors, and flow monitoring. He has several journal articles and holds several patents in his area of research.

MOHAMED LARBI ZEGHLACHE received the M.Sc. degree in reservoir engineering and field development from French Institute of Petroleum (IFP), Paris.

He is currently the Chairperson of the Researcher Development Program of the Saudi Aramco Advanced Research Centre. He is also a Senior Researcher with the Production Technology Team and the well integrity evaluation subject matter expert working on several new production and well integrity technologies. He led the well integrity logging team with the Reservoir Description and Simulation Department. Since joining Saudi Aramco, he was a Senior Petro Physicist providing expertise in formation evaluation and well placement in Ghawar carbonates and Central Arabia clastics. He has 22 years of experience in the oil and gas industry and he has worked with both Schlumberger and Halliburton, where he was a Wireline Field Engineer, a Log Analyst, and a Business Development and Technical Advisor. He has authored several SPE publications and patents.

ALI A. AL-SHAIKHI received the B.Sc. and M.Sc. degrees in electrical engineering from the King Fahd University of Petroleum and Minerals (KFUPM), Dhahran, in 1997 and 2001, respectively, and the Ph.D. degree in electrical engineering from Dalhousie University, Halifax, Canada, in 2008. He is currently the Vice President of Research & Innovation with KFUPM. He was the Chairperson of the Electrical Engineering Department and the Dean of the Engineering College, KFUPM, in 2011 and 2019, respectively. He was also the Founder and the Director of the Center for Energy and Geo-Processing (CEGP), which is a collaboration between KFUPM and Georgia Institute of Technology in seismic signal processing. He serves/served in a number of committees, such as National Power Academy (NPA), Academic Leadership Center (ALC) at MOE, Electricity Dispute Resolution Committee at ECRA, Lighting Team at SASO, and External Advisory Board of the Electrical Engineering Department, Umm Al-Qura University. His research interests include the areas of wireless communication, communication theory, digital communications, signal processing, and computer networks. He has several publications in journals, patents, and reputed conferences.

• • •